Available online at www.sciencedirect.com
ScienceDirect
Polymer 47 (2006) 7805–7812
polymer
www.elsevier.com/locate/polymer

Nano-fabrication of double gyroid network structure via ozonolysis of matrix phase of polyisoprene in poly(2-vinylpyridine)-*block*-polyisoprene films

Arimichi Okumura [a,1], Yukihiro Nishikawa [a,2], Takeji Hashimoto [a,b,*]

[a] *Hashimoto Polymer Phasing Project, ERATO, JST, Japan*
[b] *Department of Polymer Chemistry, Graduate School of Engineering, Kyoto University, Katsura, Kyoto 606-8510, Japan*

Received 1 May 2006; received in revised form 11 August 2006; accepted 11 August 2006
Available online 18 September 2006

Abstract

The film specimens having the double gyroid network structure with $Ia\bar{3}d$ space group symmetry were prepared by solution casting of poly-(2-vinylpyridine)-*block*-polyisoprene mixed with a small but varying amounts of polyisoprene with chloroform as a solvent. The network phase composed of poly(2-vinylpyridine) was first crosslinked with 1,4-diiodobutane and then the matrix phase composed of polyisoprene was degraded by ozonolysis to obtain ''free-standing'' double gyroid network texture in which the two sets of networks are interlaced without contacts with one another in vacant space via their grain boundary connections. The network structures before and after ozonolysis were investigated, respectively, by transmission electron microscopy and field-emission scanning electron microscopy with the aid of numerically calculated three-dimensional computer graphics (3d CG) of the structure. The results clarified a success of the nano-fabrication on the free-standing double gyroid structure. We propose that the 3d CG-SEM, as discussed in the text, on the morphology of the freeze-fractured surface is particularly useful for the identification of the structure.

Keywords: Nano-fabrication; Double gyroid network structure; Ozonolysis

1. Introduction

It is well-known that block copolymers form ordered domain structure such as body-centered cubic spheres, hexagonal cylinders, ordered double gyroid network structure with $Ia\bar{3}d$ space group symmetry, and lamellae. The size and shape of the domain structures can be controlled by their molecular weights and compositions. The structure units and their spacings are of the order of the radii of gyrations of the block copolymers and hence of nanometer scale [1–5].

Among these domain structures, the double gyroid network structure attracted the interest of many researchers, because the network phase and matrix phase are both continuous in 3d space as shown in Fig. 1. Fig. 1 represents computer graphics of the unit cell of the double gyroid network structure in empty space: part (a) shows a skeletal structure of the double network where two identical networks (blue and red) of the special tripod structure unit are intertwined without touching one another, and part (b) shows the network structure having the network volume fraction of 0.34 close to real block copolymer system.

In the previous work [6], the network phase was selectively degraded to create continuous and ordered nano-holes (nano-vacant-channels) in the glassy polymer matrix: this structure will be called hereafter ''the vacant double gyroid channel''. In this work we aim to create an opposite nano-texture by

* Corresponding author. Present address: Advanced Science Research Center, Japan Atomic Energy Agency, Tokai-mura, Naka-gun, Ibaraki Pref. 319-1195, Japan. Tel.: +81 29 284 3833; fax: +81 29 282 5939.
E-mail address: hashimoto@alloy.polym.kyoto-u.ac.jp (T. Hashimoto).
[1] Present address: Daicel Chemical Industries, Ltd., Corporate R&D Center, 1239 Shinzaike Aboshi-ku, Himeji, Hyogo 671-1281, Japan.
[2] Present address: Department of Macromolecular Science and Engineering, Kyoto Institute of Technology, Matsugasaki, Kyoto 606-8585, Japan.

0032-3861/$ - see front matter © 2006 Elsevier Ltd. All rights reserved.
doi:10.1016/j.polymer.2006.08.043

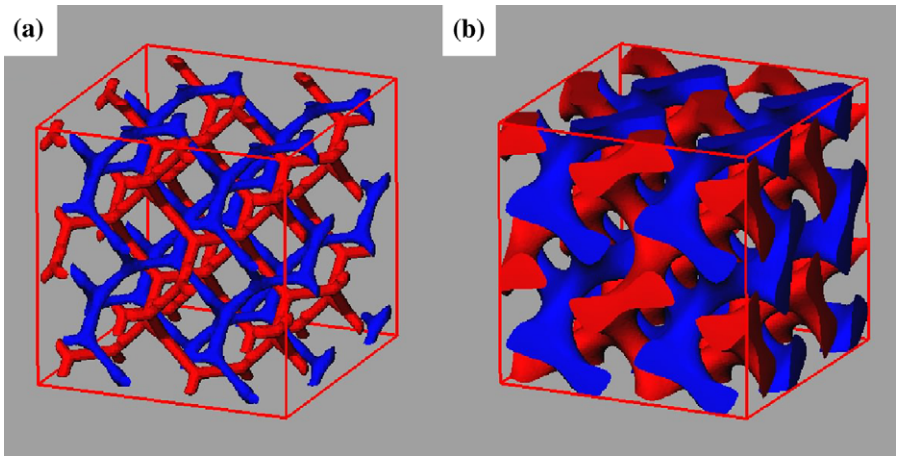

Fig. 1. Computer graphics for unit cell of double gyroid network with $Ia\bar{3}d$ space group symmetry. (a) A skeletal model and (b) a model with the network phase having volume fraction of 0.34.

selectively degrading the matrix phase, while keeping the double gyroid network phase unperturbed. We shall designate the structure thus obtained as ''the (free-standing) double gyroid network texture''.

We would like to note below some examples of excellent works previously reported. Thomas and coworkers reported UV-etched polystyrene-*block*-polyisoprene to yield a polystyrene/air double gyroid texture for an application to photonic crystal [7] and a free-standing silica-oxy-carbide network from silicon-containing block copolymer [8]. Wiesner and his coworkers reported metal oxide containing mesoporous silica with bicontinuous Plumber's Nightmare morphology [9], and mesoporous aluminosilicate materials with superparamagnetic iron oxide nanoparticles [10]. These mesoporous materials were prepared by calcination of block-copolymer-based microdomain structures.

The double gyroid network texture and/or the vacant double gyroid channels have enormous interfacial area. This unique feature may render applications of this texture (with vacancy volume fraction of 0.66) and channel (with vacancy volume fraction of 0.34) for membrane reactors, templates, filters, etc. Morphological studies of selectively degraded materials will further enrich structure characterization of the double gyroid network structures [11]. In this paper we shall report the detailed methods about preparations and characterizations of the free-standing double gyroid network composed of poly(2-vinylpyridine) (P2VP).

2. Experimental methods

2.1. Polymers and film preparation

In this study, we used a block copolymer system composed of a binary mixture of poly(2-vinylpyridine)-*block*-polyisoprene diblock copolymer (P2VP-*b*-PI) and homopolyisoprene (HPI), designated hereafter as P2VP-*b*-PI/HPI. The block copolymer was polymerized by living anionic polymerization with *sec*-butyllithium as an initiator and tetrahydrofuran as a solvent. Polyisoprene block chains have a microstructure with 1,4- and vinyl-linkages (1,2-linkage plus 3,4-linkage) of 16 and 84%, respectively, as determined by ^{1}H NMR. The P2VP-*b*-PI block copolymer has a total number average molecular weight (M_n) of 6.7×10^4 with weight fraction 0.39 of polyisoprene block chains. The HPI has $M_n = 4 \times 10^3$. The homopolymer was polymerized by living anionic polymerization with *sec*-butyllithium as an initiator and hexane as a solvent. The HPI chains have a microstructure with 1,4- and 3,4-linkages of 85 and 15%, respectively, as determined by ^{1}H NMR. The P2VP-*b*-PI and HPI were mixed so that the mixtures had an overall volume fraction of PI units from 0.60 to 0.70 with an increment of 0.02.

The mixtures of P2VP-*b*-PI/HPI were dissolved in ca. 5 wt% total polymer concentration with benzene. Thin film specimens about 1 mm thick containing the varying total PI volume fractions were prepared from the solution in a Petri dish by slowly evaporating the solvent over approximately a month. The as-cast films were further dried under vacuum for about a week until constant weight was attained.

2.2. Selective crosslinking and staining of network texture with DIB

1,4-Diiodobutane (DIB) is used to selectively crosslink and stain the P2VP network phase. For this purpose as-cast films were exposed to DIB vapor at 80 °C for 72 h. The color of the film was changed from transparent to yellowish. The film was dried under vacuum at 80 °C for 48 h.

2.3. Ozonolysis of matrix phase of texture

Ozonolysis was used to selectively degrade the PI matrix. To cleave the carbon–carbon double bond of the PI block in P2VP-*b*-PI as well as PI homopolymers mixed, the DIB crosslinked film was soaked in heptane solution and ozone was bubbled in heptane solution for 48 h at room temperature. The cleaved compounds were leached out from the films by soaking them in ethanol at room temperature for 24 h in order to obtain double gyroid textures of P2VP chains.

2.4. Characterization of texture

The microdomain structure in the as-cast film was observed under a transmission electron microscope (TEM, JEOL JEM-2000FXZ) operated at 120 kV on the ultrathin sections obtained with a Reichert-Nissei Ultracut-S ultramicrotome. Prior to ultramicrotoming the specimens, they are stained with OsO_4 vapor for 30 min.

The double gyroid network texture comprising of the P2VP microdomain created after the DIB crosslinking of the P2VP microdomains and ozonolysis of PI matrix phase was investigated under the field-emission scanning electron microscopy (FE-SEM, Hitachi S-900S) operated at 20 kV. For this purpose the film subjected to the ozonolysis was freeze-fractured according to the conventional method, and the fracture surfaces were subsequently sputter-coated with platinum by Hitachi E-1030 ion sputter for FE-SEM observation.

3. Results and discussion

3.1. Preparation and characterization of double gyroid network texture

The double gyroid network texture can be developed only for a very narrow composition range of the block copolymer. Therefore a precise control of composition of the block copolymer is required to obtain the texture. We could overcome this difficulty by blending an appropriate amount of a homopolymer with a block copolymer. In this paper, we used P2VP-*b*-PI that has a PI composition in the block copolymer smaller than that expected for the gyroid structure to prepare the mixtures P2VP-*b*-PI/HPI.

Fig. 2 shows the TEM micrographs of a series of the as-cast specimens with decreasing total volume fraction of P2VP: (a) 0.36, (b) 0.34, (c) 0.32, and (d) 0.30. The specimens were first exposed to DIB for crosslinking and staining the P2VP double gyroid networks and then ultrathin-sectioned. The dark and bright phases in the TEM images correspond to the stained P2VP and unstained PI phase. Fig. 2a shows the ordered lamella phase. Fig. 2c and d shows the P2VP cylinder structure in the matrix of PI, while Fig. 2b shows seemingly the ordered double gyroid network texture. Therefore the double gyroid structure of P2VP was found in very narrow composition range of P2VP between 0.36 and 0.32, which corresponds to weight fraction of HPI between 30 and 44. In the following sections we have investigated the detail of the structure shown in Fig. 2b.

Fig. 3 shows TEM for the as-cast films before the DIB treatment having total P2VP volume fraction of 0.34. The images were obtained with ultrathin sections stained with OsO_4. Two different types of structures can be observed in the low

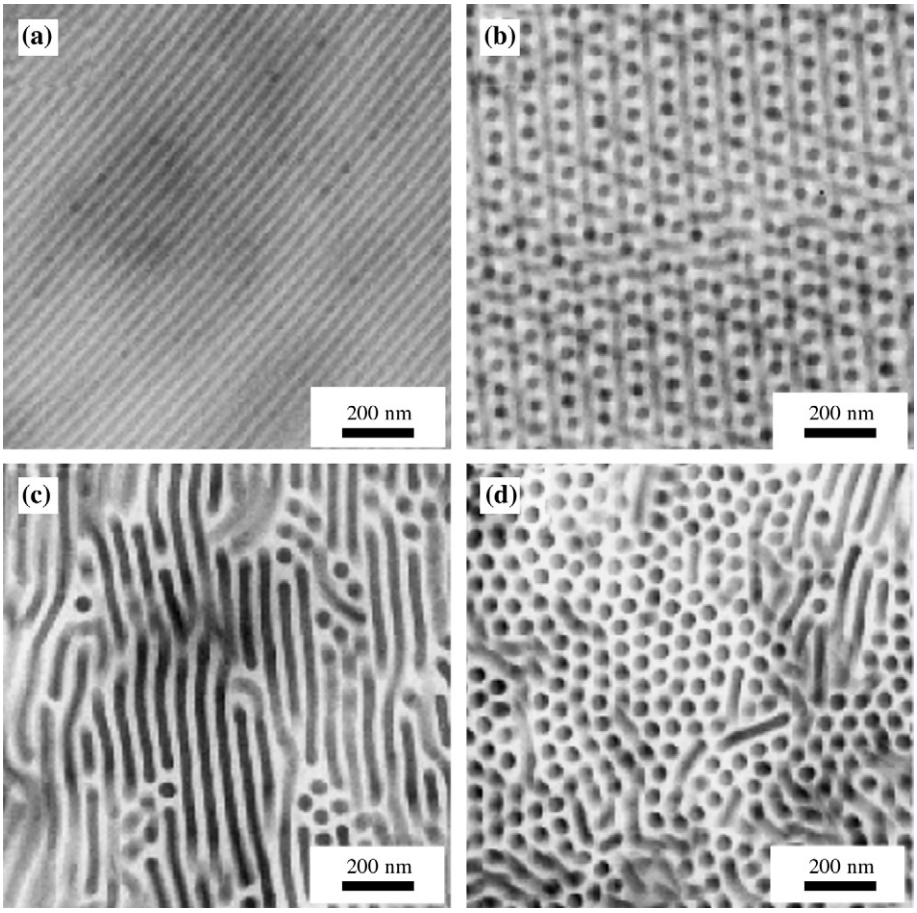

Fig. 2. TEM images for as-cast film having total P2VP volume fraction of (a) 0.36, (b) 0.34, (c) 0.32 and (d) 0.30 subjected to the DIB treatment described in the text. The dark and bright phases are the P2VP and PI phases stained and unstained with DIB, respectively.

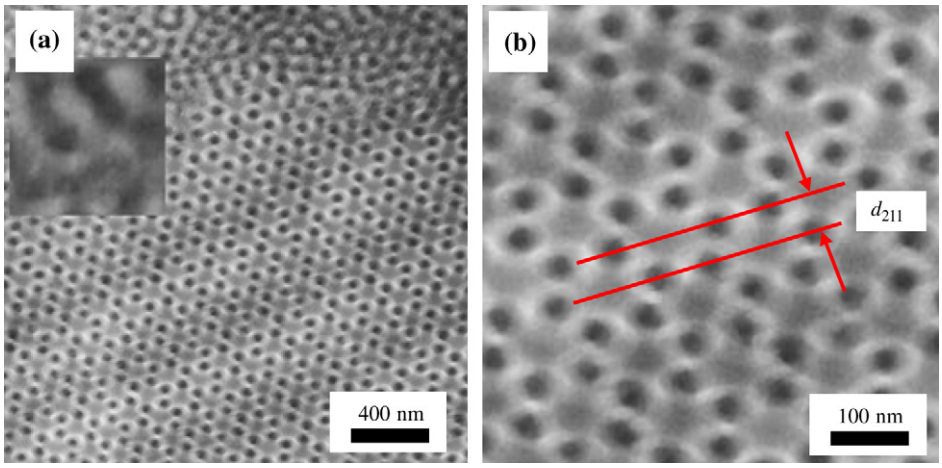

Fig. 3. TEM images for as-cast films of P2VP-*b*-PI having total P2VP volume fraction of 0.34 untreated with DIB. Both low (a) and high magnification images (b) were obtained on the ultrathin sections stained with OsO_4 vapor. The inset in part (a) magnifies the distorted ordered structure (sponge-like structure) which exists in the grain boundary regions of the ordered structure, as shown in the upper edge of the image in part (a).

magnification TEM shown in Fig. 3a. One is an ordered structure, and the other is a disordered structure that exists in grain boundary regions between ordered structures, as shown in the upper right corner of the image in part (a). Fig. 3b shows a high magnification micrograph for a part of the ordered structure shown in part (a), while the inset to Fig. 3a shows a high magnification micrograph of a part of the disordered structure. The disordered structure has the characteristic of the so-called sponge-like structure, the 3d bicontinuous structure, found in phase-separating polymer blends [12]. The ordered structure has a characteristic of wagon-wheel-like structure in which a central gray shaft (or core) is surrounded by (i) six dark spots and (ii) six gray spokes. The ordered grains have the size of a few ten micrometers or more.

We analyzed whether or not the observed ordered structure shown in Fig. 3b fits the ordered double gyroid network structure. The analysis involves a comparison of the TEM image for the ordered structure shown in Fig. 3b with the TEM image, which we shall define as CG-TEM image (computer graphics of TEM image), numerically constructed on the basis of the differential geometry on the minimal surface of the gyroid. As described elsewhere [11,13], the double gyroid network structure with a volume fraction of the network phase of 0.34 was constructed by applying the parallel surface method to the minimal surface of the gyroid which was approximated by trigonometric functions. Fig. 4a defines the Cartesian coordinate of the unit cell of the double gyroid network structure shown in Fig. 1b in order to construct CG-TEM image.

We first binarized the contrast of the gyroid structure in such a way that matrix phase (corresponding to the stained PI phase) is dark and the network phase (corresponding to the unstained P2VP phase) bright. The double gyroid structure was cut parallel to various crystallographic planes (*hkl*) at various positions along *x*-axis,

$$h(x - x_0) + ky + lz = 0 \tag{1}$$

where x_0 is the intercept of the plane with *x*-axis, and x_0, *x*, *y*, and *z* are reduced with respect to length of cell edge. Then the gray contrast of the ultrathin section with thickness *t* reduced with respect to length of cell edge, viewed along the normal direction of (*hkl*) plane, was numerically calculated for a set of variables

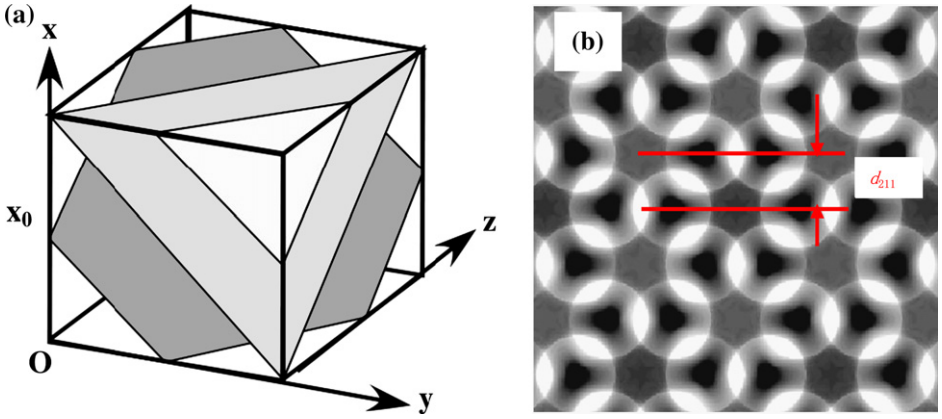

Fig. 4. (a) Definition of Cartesian coordinate O*xyz* and origin O in the unit cell containing the double gyroid network structure with $Ia\bar{3}d$ space group symmetry for the construction of the CG-TEM images, and (b) the CG-TEM image for the double gyroid network structure for the ultrathin section parallel to (111) plane at $x_0 = 0$ and with thickness $t = 0.9$.

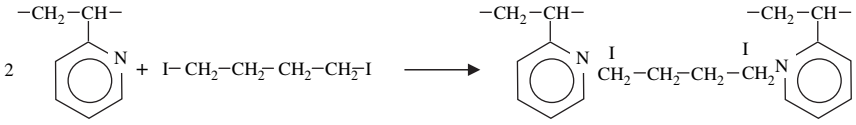

Scheme 1.

indicating (1) type of the plane (*hkl*), (2) position x_0, and (3) thickness t of the thin sections in order to compare the calculated CG-TEM images with the observed TEM images.

Fig. 4b shows the CG-TEM image which gives a best fit with the observed TEM image shown in Fig. 3b. The calculated image was obtained for (111) plane with $x_0 = 0$ and $t = 0.9$ and satisfies all the three characteristics of the wagon wheel pattern. A good agreement between the calculated and observed images indicates that the observed image is consistent with the double gyroid network structure, though other possible structures cannot be completely ruled out only by this image. Fig. 4b indicates the (211) crystallographic plane spacing d_{211}. The d_{211} spacing measured from Fig. 3b was about 71 nm.

3.2. Fabrication to obtain free-standing double gyroid network texture

3.2.1. Crosslinking with DIB

As-cast films were treated with DIB vapor at 80 °C for 72 h. Scheme 1 shows expected crosslinking mechanism. The nitrogen atom in the P2VP aromatic ring tends to be negatively charged and the two carbons at 1 and 4 positions in 1,4-diiodobutane tend to be positively charged. These nitrogens and carbons may create strong bondings. As DIB has two positively charged carbons, a single DIB molecule can connect two different nitrogens, which are either in the same polymer chain or in different polymer chains as shown in Scheme 1.

Table 1
Efficiency of the DIB crosslinking and ozonolysis reaction

	As-cast film	After DIB crosslink	After ozonolysis
Film A	1	1.526	1.107
Film B		1.539	1.104
Calculated		1.568	0.957
Efficiency of reaction	–	0.93–0.95	0.70

After the DIB treatment, the weight change in the film was investigated for two test films designated A and B, and the results are summarized in Table 1. After the DIB treatment, weights of the films A and B were 1.526 and 1.539 times of the as-cast film, respectively. If all pyridine rings create the bonding with the DIB, the weight of the DIB treated film should be 1.568 times of the as-cast film for a given blend composition and block copolymer composition. From this estimation, efficiency of DIB crosslinking is estimated to be $94 \pm 1\%$ as summarized in Table 1.

3.2.2. Ozonolysis

Degradation of double bond in polyisoprene with ozone is discussed and reported in many literature works [14]. Degradation of 1,2- or 3,4-isomer of polyisoprene with ozone increases the weight of the polymer, while degradation of 1,4-isomer with ozone degrades the polymer chain, as shown in Scheme 2.

As the living anionic polymerization of the block copolymer was done in a polar solvent of THF, the PI block chains had a low content of 1,4-linkage: the compositions of the 1,2-, 3,4-, and 1,4-microstructures of the PI were 24, 60, and 16%, respectively. Thus cleaving of PI main chain in the block copolymer is expected to happen in every 6.25 repeating isoprene monomer unit on average. If the ozone degradation reaction proceeds with 100% efficiency, then the weight of the degraded film becomes 0.957 times the weight of the undegraded as-cast film. Thus we can estimate the weight fraction of PI degraded with the ozone treatment with respect to the total amount of PI in P2VP-*b*-PI/HPI by measuring the weight change with the reaction. In this estimation, we assumed that all homo PI chains were removed from the system by washing it with heptane after ozonolysis, independent of a degree to which homo PI chains were degraded. The results of a long time treatment with ozone (about 100 h) are listed in Table 1. Fig. 5 shows the weight fraction of the degraded PI as a function of time. The result shows that the weight fraction reached a constant value of 0.75 after

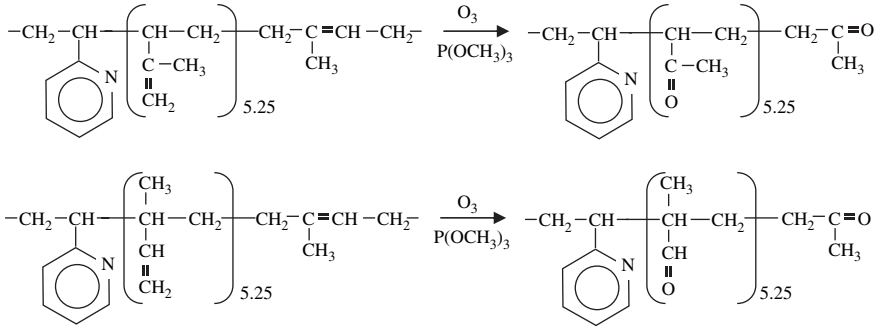

Scheme 2.

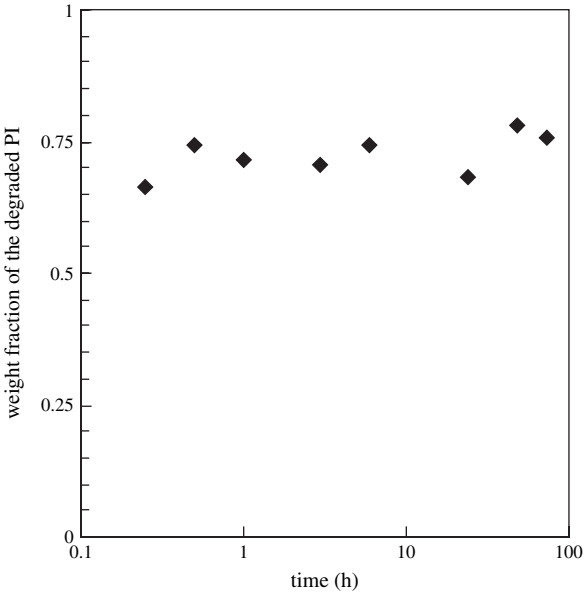

Fig. 5. Change in weight fraction of the degraded PI, with respect to the total amount of PI in the system, with time, subjected to ozonolysis.

3 h. This value hardly changed for the prolonged degradation time up to 72 h.

3.3. Morphological characterization of the texture after ozonolysis

The texture obtained after the nano-fabrication as discussed in Section 3.2 was investigated with FE-SEM on the freeze-fractured surface. We found that the ultramicrotoming to prepare ultrathin sections for the TEM observation easily caused deformation of the texture. Therefore we believe the FE-SEM method is superior to the TEM method for this texture. The results are shown in parts (a) and (b) of Fig. 6 with a low and high magnification, respectively. The part (a) shows a uniform morphology over a wide area. Investigation of many images showed that the average grain size is about several tens of micrometers. The enlarged image shown in part (b) suggests a local surface topography created by a fracture of the gyroid texture on a particular plane parallel to a particular crystallographic plane [13]. The roughness of the fractured surface observed at a large length scale, shown by the image in part (a), may reflect the cleavage surfaces with different step heights [15]. The part (b) shows a regular periodic pattern composed of the texture that appeared on the fracture surface (bright) and its interstitial vacant space (dark).

Fig. 7 shows two types of the FE-SEM images (parts (a) and (b)) which were frequently observed on the fractured surfaces and their corresponding calculated images in parts (c) and (d), respectively. The image in Fig. 7a is similar to that in Fig. 6b.

The calculated images, defined as CG-SEM image, were obtained in a manner similar to that for CG-TEM images. The images in parts (c) and (d) represent 2d cross-sectional CG-TEM images of the texture cut parallel to (100) plane at $x_0 = 0.2$ and (110) plane at $x_0 = 0.12$, respectively. The images are binarized such that the texture appearing on the cross-sectional plane is represented bright and the interstitial vacancy dark. This binarization involves an over simplification of the FE-SEM image, because it ignores fine topographical features of the FE-SEM images along the depth direction with respect to the fracture surface. Nevertheless, the observed and predicted images are in good agreement [15], at least qualitatively. This fact elucidates that the texture obtained after the ozonolysis is really the free-standing double gyroid texture composed of the crosslinked P2VP block chains and that the ozonolysis selectively degraded the matrix phase, while keeping the double gyroid network structure essentially unaltered. The bright band running nearly along the horizontal direction in the middle of the image in part (a) may indicate a region protruded with respect to other areas of the fractured surface.

The spacings drawn in parts (a) and (b) correspond to a and $2a/\sqrt{6}$, respectively, where a is the cell edge of the cubic unit cell. As $a = \sqrt{6}\, d_{211}$, and d_{211} was measured to be about 71 nm in Fig. 3b, a is estimated to be about 174 nm. Therefore these spacings in parts (a) and (b) should be equal to about 174 nm and 142 nm, respectively. The observed spacings are about 174 nm and 189 nm in parts (a) and (b), respectively, consistent with the above expected values, though the latter value

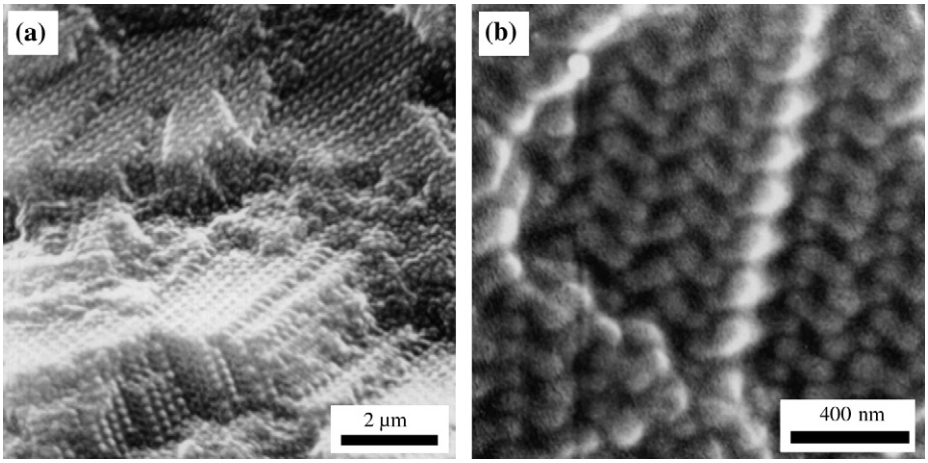

Fig. 6. FE-SEM images on the fractured surface of the ozone-degraded films: (a) low and (b) high magnifications.

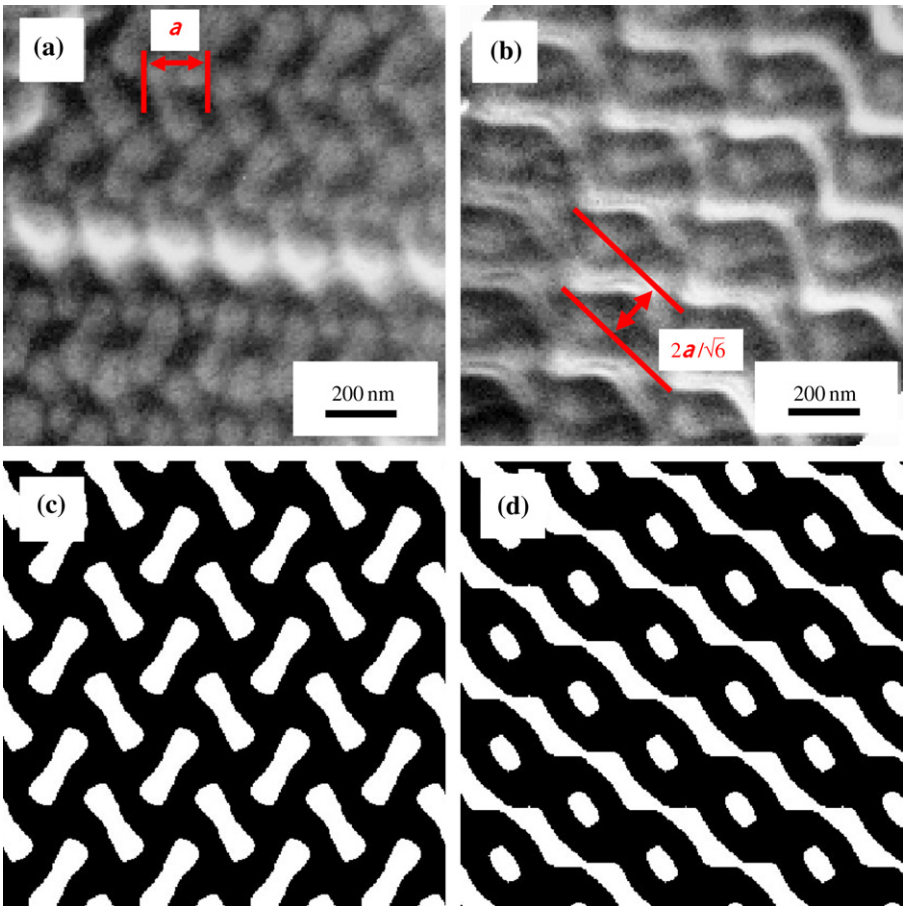

Fig. 7. Frequently observed two kinds of FE-SEM images (parts (a) and (b)) and their corresponding 2d CG-SEM images cut parallel to (100) plane at $x_0 = 0.2$ (part (c)) and (110) plane at $x_0 = 0.12$ (part (d)).

is larger than the expected value, probably due to some distortions of the structure.

It is important for us to discern some quantitative differences between the experimental FE-SEM images, as shown in Fig. 7a and b, and the 2d CG-SEM images on the fractured surfaces parallel to the particular crystallographic planes, as shown in Fig. 7c and d. We believe that this difference arises from the fact that the FE-SEM images reflect topographical features along depth directions of the fractured surfaces, while the oversimplified 2d CG-SEM images disregard the features.

Fig. 8a and b represents calculated 3d CG-SEM images of the texture cross-sectioned parallel to (100) at $x_0 = 0.2$ and

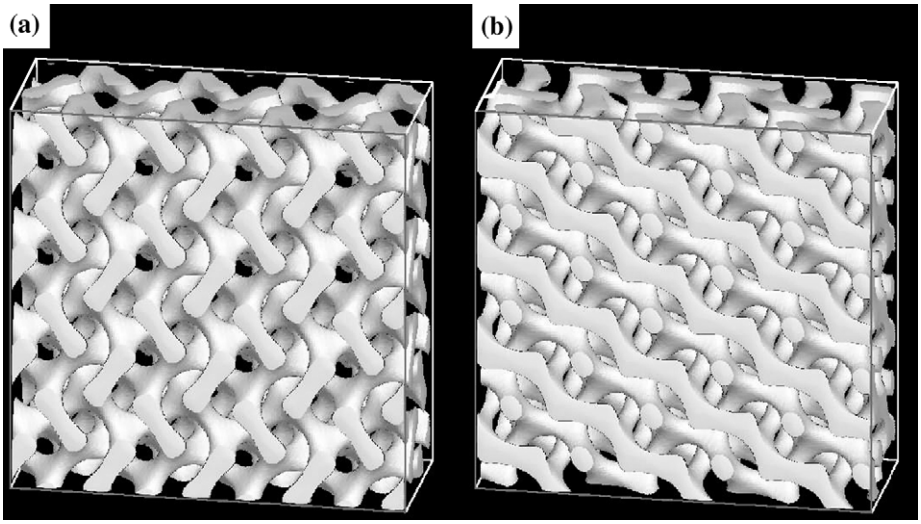

Fig. 8. Three-dimensional cross-sectional CG-SEM images cut parallel to (a) (100) plane at $x_0 = 0.2$ and (b) (110) plane at $x_0 = 0.12$.

(110) planes at $x_0 = 0.12$, respectively. The 3d CG-SEM images quantitatively illuminate the topographical features of the double gyroid texture around the cross-sectional planes, revealing fine structures along the depth directions across the cross-sectional plane. In fact, Fig. 7a is more similar to Fig. 8a than to Fig. 7c, and Fig. 7b is more similar to Fig. 8b than to Fig. 7d. The results reveal themselves, the importance of the 3d CG-SEM images. Comparisons of the calculated 3d images of the cross-sections with FE-SEM images with an improved image quality and resolution would allow us to characterize topographical features of the real double gyroid texture more precisely, which will deserve future studies.

4. Summary

The film specimens comprising of poly(2-vinylpyridine)-*block*-polyisoprene (P2VP-*b*-PI) and homopolyisoprene having the double gyroid network structure were subjected to the nano-fabrication processes to prepare the ''free-standing'' double gyroid network in vacant space. The nano-fabrication involves: first (1) crosslinking of the double gyroid network phase of P2VP with 1,4-diiodobutane, followed by (2) ozone degradation of the matrix PI phase. The double gyroid network structure in the as-cast films was firmly confirmed by TEM with numerically constructed computer graphics (CG-TEM) based on differential gyometry of the double gyroid structure with $Ia\bar{3}d$ space group symmetry. The structure after the nano-fabrication was confirmed again by FE-SEM images obtained together with the 3d computer graphics (3d CG-SEM). The double networks are expected to be free-standing through the interconnection of the networks at the grain boundary regions.

Acknowledgement

This work was supported in part by a grant from 21st century COE program, COE for a United Approach to New Materials Science.

References

[1] Sadron C, Gallot B. Makromol Chem 1973;164:301–32.
[2] Hashimoto T, Shibayama M, Fjimura M, Kwai H. In: Meier DJ, editor. Block copolymer science and technology. New York: MMI Press/ Harwood Academic; 1983. p. 63–108.
[3] Thomas EL, Alward DB, Kinning DJ, Martin DC, Handlin DL, Fetters LJ. Macromolecules 1986;19:2197–202; Hasegawa H, Tanaka H, Yamasaki K, Hashimoto T. Macromolecules 1987;20: 1651–62.
[4] Hajduk DA, Harper PE, Gruner SM, Honecker CC, Kim G, Thomas EL, et al. Macromolecules 1994;27:4063–75.
[5] Hamley I. The physics of block copolymers. Oxford: Oxford Univ. Press; 1988.
[6] Hashimoto T, Tsutsumi K, Funaki Y. Langmuir 1997;13:6869.
[7] Urbas M, Maldovan M, DeRege P, Thomas EL. Adv Mater 2002;14: 1850.
[8] Chan VZ-H, Hoffman J, Lee VY, Itarou H, Averopoulas A, Hadjichristidis N, et al. Science 1999;286:1716.
[9] Finnefrock AC, Ulrich R, Du Chesne A, Unger KK, Gruner SM, Wiesner U. Angew Chem Int Ed 2001;40:1208.
[10] Garcia C, Zhang Y, DiSalvo F, Wiesner U. Angew Chem Int Ed 2003;42: 1526.
[11] Hashimoto T, Nishikawa Y, Tsutsumi K. Macromolecules. Submitted for publication.
[12] Jinnai H, Koga T, Nishikawa Y, Hashimoto T, Hyde ST. Phys Rev Lett 1997;78:2248; Nishikawa Y, Jinnai H, Koga T, Hashimoto T, Hyde ST. Langmuir 1998;14:1242.
[13] Nishikawa Y. Ph.D. thesis presented to Graduate School of Engineering, Kyoto University, 1999.
[14] Ho KW. J Polym Scit Part A Polym Chem Ed 1986;24:241–53.
[15] Among many 2d cross-sectional CG-TEM images of the texture cut parallel to various crystallographic planes at various x_0 values that we have investigated, the images cut parallel to (100) plane at $x_0 = 0.2$ (Fig. 7c) and (110) plane at $x_0 = 0.12$ (Fig. 7d) are almost similar to the FE-SEM images shown in Fig. 7a and b, respectively. However, we do not claim that these planes are the cleavage planes for the texture. The cleavage planes for the double gyroid network texture which exists in the voided matrix are still left unsolved. In the case of the complementary texture in which only double gyroid network domains are made into a vacant phase, the plane parallel to the (211) plane is indicated to be a cleavage plane [6,11]. However, for the present texture (free-standing double gyroid network texture), 2d cross-sectional images cut parallel to (211) plane did not show naturally any similarity to the observed FE-SEM images.